

# Optimized Schwarz algorithms in the framework of DDFV schemes

Martin J. Gander<sup>1</sup>, Florence Hubert<sup>2</sup>, and Stella Krell<sup>3</sup>

## 1 Introduction

We are interested in this paper in anisotropic diffusion problems of the form

$$-\operatorname{div}(A\nabla u) = f \text{ on } \Omega; \quad u = 0 \text{ on } \partial\Omega. \quad (1)$$

A discretization of the Schwarz algorithm using Discrete Duality Finite Volume methods (DDFV for short) for such problems was developed in [3]. The DDFV method needs a dual set of unknowns located on both vertices and “centers” of the primal control volumes, which leads to two meshes, the primal and the dual one, and permits the reconstruction of two-dimensional discrete gradients located on a third partition of  $\Omega$ , called the diamond mesh, and also a discrete divergence operator defined by duality. The DDFV method is particularly accurate in terms of gradient approximation, see the benchmark [11] for problem (1) and an extensive bibliography. DDFV methods are also very robust, see [6, 2] for theoretical justifications, and [5] for applications. It is therefore of great interest to develop parallel solvers for such discretizations.

A non-overlapping Schwarz method using Robin transmission conditions was first proposed at the continuous level by Lions in [12]. For the model problem (1), the algorithm with two non-overlapping subdomains,  $\Omega = \Omega_1 \cup \Omega_2$ , and interface  $\Gamma = \partial\Omega_1 \cap \partial\Omega_2$ , computes for iteration index  $l \in \mathbb{N}^*$  the subdomain solutions

$$\begin{aligned} -\operatorname{div}(A\nabla u_j^l) &= f \quad \text{on } \Omega_j, & u_j^l &= 0 & \text{on } \partial\Omega_j \cap \partial\Omega, \\ A\nabla u_j^l \cdot \mathbf{n}_{ji} + pu_j^l &= -A\nabla u_i^{l-1} \cdot \mathbf{n}_{ij} + pu_i^{l-1} & \text{on } \Gamma, & j \neq i, \end{aligned} \quad (2)$$

where  $\mathbf{n}_{ji}$  is the unit normal from  $\Omega_j$  to  $\Omega_i$ , and  $p$  is a parameter that one can choose to accelerate convergence. Choosing  $p$  such that the algorithm converges as fast as possible leads to a so called optimized Schwarz method [8].

The non-overlapping algorithm ((2)) at the discrete level is interesting for coupling non-matching grids, see for example [1], [4] and [9] for isotropic diffusion problems or [10], [7] for general diffusion. It has also been analyzed in [3] in the case of highly anisotropic operators, and on a wide range of meshes. Numerical experiments in [3] showed however that the DDFV discretization chosen at the interfaces leads to a convergence factor of  $1 - \mathcal{O}(h)$  of the algorithm ( $h$  denotes the

---

<sup>1</sup> University of Geneva, 2-4 rue du Lièvre CP 64 1211 Genève Switzerland e-mail: martin.gander@unige.ch <sup>2</sup> Aix-Marseille Université, LATP, 39 rue F. Joliot Curie 13 453 Marseille cedex 13, FRANCE e-mail: florence.hubert@univ-amu.fr <sup>3</sup> Université de Nice, Parc Valrose 28 avenue Valrose 06108 Nice Cedex 2 FRANCE e-mail: krell@unice.fr

mesh size), when the parameter  $p$  was chosen numerically such that convergence was fastest. This contraction factor is much worse than the optimal contraction factor  $1 - \mathcal{O}(\sqrt{h})$  of ((2)) for other discretizations, see [8]. The purpose of this short paper is to investigate why the classical DDFV discretization leads to such a slow convergence of the optimized Schwarz method, and to develop a new discretization of the transmission conditions in order to restore the optimal convergence rate. We show our results for the Poisson equation,  $A = \text{Id}$ , but the extension to anisotropic tensors  $A$  can be obtained similarly. In Section (2), we show for the case of the Poisson equation and square meshes on half spaces that the traditional DDFV discretization leads to a mass matrix in the term with the Robin parameter. This mass matrix couples the primal and dual grids, and destroys the good convergence behavior of the optimized Schwarz method. In Section (3), we then show how to discretize the transmission conditions differently in the context of DDFV in order to recover the optimal convergence factor  $1 - \mathcal{O}(\sqrt{h})$ . We then extend the algorithm to general meshes and prove convergence. Finally, in Section (4), we present numerical experiments which illustrate our analysis.

## 2 DDFV discretization of the optimized Schwarz algorithm

We decompose  $\Omega := \mathbb{R}^2$  into two non-overlapping half planes  $\Omega_1 := (-\infty, 0) \times \mathbb{R}$  and  $\Omega_2 := (0, \infty) \times \mathbb{R}$ , with the interface  $\Gamma := \partial\Omega_1 \cap \partial\Omega_2$ . We use a regular grid of squares, so that the DDFV discretization away from the interface  $\Gamma$  leads to two interlaced five point finite difference schemes. The mesh size is denoted by  $h$ . We use for the scheme aligned with the interface star indices, and for the other one indices without stars, see Figure (1). The DDFV Schwarz algorithm proposed in [3] solves at each iteration  $l \in \mathbb{N}^*$ , on each domain  $j$  on interior primal cells

$$u_{m+1,n}^{j,l} - 2u_{m,n}^{j,l} + u_{m-1,n}^{j,l} + u_{m,n+1}^{j,l} - 2u_{m,n}^{j,l} + u_{m,n-1}^{j,l} = 0, m > 0. \quad (3)$$

In order to obtain (3) for  $m = 1$ , we introduce  $u_{0,n}^{j,l}$  which is linked with the interface primal unknowns  $u_{\frac{1}{2},n}^{j,l}$  by

$$u_{\frac{1}{2},n}^{j,l} = \frac{1}{2}(u_{1,n}^{j,l} + u_{0,n}^{j,l}). \quad (4)$$

On interior dual cells, the algorithm solves

$$u_{m^*+1,n^*}^{j,l} - 2u_{m^*,n^*}^{j,l} + u_{m^*-1,n^*}^{j,l} + u_{m^*,n^*+1}^{j,l} - 2u_{m^*,n^*}^{j,l} + u_{m^*,n^*-1}^{j,l} = 0, m^* > 0, \quad (5)$$

whereas on boundary dual cells, the additional fluxes  $\varphi_{n,n^*}^{j,l}$  are used,

$$u_{1^*,n^*}^{j,l} - u_{0^*,n^*}^{j,l} + \frac{1}{2}(u_{0^*,n^*+1}^{j,l} - 2u_{0^*,n^*}^{j,l} + u_{0^*,n^*-1}^{j,l}) + \frac{h}{2}(\varphi_{n-1,n^*}^{j,l} + \varphi_{n,n^*}^{j,l}) = 0. \quad (6)$$

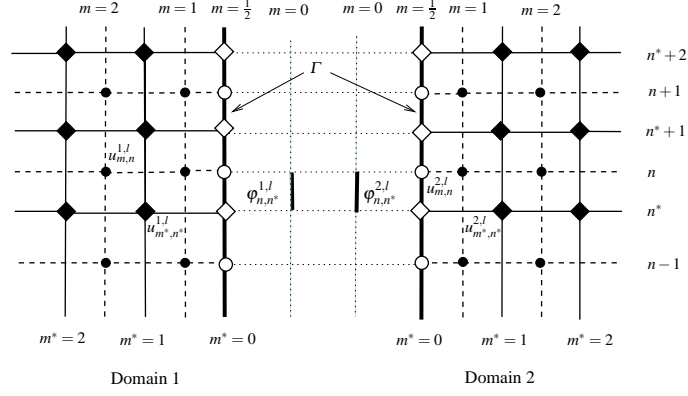


**Fig. 1** The unknowns  $u_{m,n}^{j,l}$  are associated with the primal cells, whose centers are bullets  $\bullet$ ; the unknowns  $u_{m^*,n^*}^{j,l}$  are associated with the dual cells shown in dashed, whose centers are diamonds  $\diamond$ , or  $\diamond$  for boundary cells. The centers of the dual cells  $\diamond$  are the vertices of the primal cells, and similarly the centers of the primal cells  $\bullet$  are the vertices of the dual cells. Additional primal unknowns  $u_{\frac{1}{2},n}^{j,l}$ , located at  $\circ$ , and also additional flux unknowns  $\varphi_{n,n^*}^{j,l}$  are needed on the interface  $\Gamma$ . The indices  $j$  and  $l$  stand for the domain and the iteration.

The Robin transmission condition on  $\Gamma$  can now be expressed using the fluxes  $\varphi_{n,n^*}^{j,l}$ ,

$$\varphi_{n,n^*}^{j,l} + \frac{p}{2}(u_{0^*,n^*}^{j,l} + u_{\frac{1}{2},n}^{j,l}) = -\varphi_{n,n^*}^{j,l-1} + \frac{p}{2}(u_{0^*,n^*}^{j,l-1} + u_{\frac{1}{2},n}^{j,l-1}). \quad (7)$$

Finally, a consistency condition is required for the fluxes, namely

$$\frac{1}{2}(\varphi_{n,n^*}^{j,l} + \varphi_{n,n^*+1}^{j,l}) = \frac{2}{h}(u_{\frac{1}{2},n}^{j,l} - u_{1,n}^{j,l}). \quad (8)$$

Equations (3)-(8) completely describe the original DDFV Schwarz algorithm from [3]. In order to analyze the DDFV discretization of the optimized Schwarz algorithm (3) and (5), we perform a discrete Fourier transform in the  $n$  index, which corresponds to the  $y$  variable, aligned with the interface. Setting  $u_{m,n}^{j,l} = \hat{u}_{m,k}^{j,l} e^{iknh}$ ,  $u_{m^*,n^*}^{j,l} = \hat{u}_{m^*,k}^{j,l} e^{ikn^*h}$ , both  $\hat{u}_{\cdot,k}^{j,l}$  and  $\hat{u}_{(\cdot)^*,k}^{j,l}$  satisfy the recurrence relation

$$X_{m+1} - 2X_m + X_{m-1} + \alpha_k X_m = 0, \quad (9)$$

with  $\alpha_k = 2 \cos kh - 2$ . The general solutions of (3) and (5) are bounded solutions of (9), which implies that

$$\hat{u}_{m,k}^{j,l} = C_k^{j,l} \lambda^m, \quad \hat{u}_{m^*,k}^{j,l} = C_k^{*,j,l} \lambda^{m^*}, \quad \lambda := \frac{2 - \alpha_k - \sqrt{(2 - \alpha_k)^2 - 4}}{2}.$$

In order to determine the constants  $C_k^{j,l}$  and  $C_k^{*,j,l}$  from the transmission conditions (6) and (8), we eliminate the fluxes from the interface conditions using (7):

$$\begin{aligned} & \frac{1}{h}(u_{0^*,n^*}^{j,l} - u_{1^*,n^*}^{j,l}) - \frac{1}{2h}(u_{0^*,n^*+1}^{j,l} - 2u_{0^*,n^*}^{j,l} + u_{0^*,n^*-1}^{j,l}) + p\gamma_{n^*}(u^{j,l}) \\ &= -\frac{1}{h}(u_{0^*,n^*}^{i,l-1} - u_{1^*,n^*}^{i,l-1}) + \frac{1}{2h}(u_{0^*,n^*+1}^{i,l-1} - 2u_{0^*,n^*}^{i,l-1} + u_{0^*,n^*-1}^{i,l-1}) + p\gamma_{n^*}(u^{i,l-1}), \end{aligned}$$

and

$$\frac{2}{h}(u_{\frac{1}{2},n}^{j,l} - u_{1,n}^{j,l}) + p\gamma_n(u^{j,l}) = -\frac{2}{h}(u_{\frac{1}{2},n}^{i,l-1} - u_{1,n}^{i,l-1}) + p\gamma_n(u^{i,l-1}),$$

with traces

$$\gamma_{n^*}(u^{j,l}) = \frac{1}{4}(u_{\frac{1}{2},n}^{j,l} + 2u_{0^*,n^*}^{j,l} + u_{\frac{1}{2},n-1}^{j,l}), \quad \gamma_n(u^{j,l}) = \frac{1}{4}(u_{0^*,n^*}^{j,l} + 2u_{\frac{1}{2},n}^{j,l} + u_{0^*,n^*+1}^{j,l}). \quad (10)$$

We then obtain for the iteration of the constants using (4),  $\begin{pmatrix} C_k^{j,l} \\ C_k^{*,j,l} \end{pmatrix} = B \begin{pmatrix} C_k^{i,l-1} \\ C_k^{*,i,l-1} \end{pmatrix}$

with the iteration matrix  $B = M^{-1}N$ , where

$$\begin{aligned} M &= \begin{pmatrix} \frac{1}{h}(1-\lambda) + \frac{p}{4}(1+\lambda) & \frac{p}{4}(1+e^{ikh}) \\ \frac{p}{8}(1+\lambda)(1+e^{-ikh}) & \frac{1}{h}(1-\lambda) - \frac{\alpha_k}{2h} + \frac{p}{2} \end{pmatrix} \\ N &= \begin{pmatrix} -\frac{1}{h}(1-\lambda) + \frac{p}{4}(1+\lambda) & \frac{p}{4}(1+e^{ikh}) \\ \frac{p}{8}(1+\lambda)(1+e^{-ikh}) & -\frac{1}{h}(1-\lambda) + \frac{\alpha_k}{2h} + \frac{p}{2} \end{pmatrix}. \end{aligned}$$

**Proposition 1.** *The optimized parameter in the DDFV discretized Schwarz algorithm ((3)-(8)) satisfies  $p_{opt} = \text{Argmin}_p \max_k(\rho(B)) = \frac{4}{h}$ , and the associated optimized contraction factor is  $1 - \frac{1}{2}k_{\min}h + O(h^2)$ .*

*Proof.* The proof of this result is based on two observations: the minimum is obtained when both eigenvalues are the same, which is achieved with the given choice of  $p$ , and then the maximum is attained for the lowest mode  $k = k_{\min}$ . The computations are however too long and technical for this short paper.

### 3 A new DDFV Discretization of the Transmission Conditions

A careful comparison with the convergence results in [8] suggests that the mass matrices appearing in the traces  $\gamma_n(u^{j,l})$  introduce an additional coupling, which prevents the optimized DDFV Schwarz algorithm from converging rapidly. Modifying the traces  $\gamma_{n^*}(u^{j,l})$  in (10) to be lumped, i.e.

$$\gamma_{n^*}^{\text{new}}(u^{j,l}) = u_{0^*,n^*}^{j,l}, \quad \gamma_n^{\text{new}}(u^{j,l}) = u_{\frac{1}{2},n}^{j,l}, \quad (11)$$

the iteration matrix becomes diagonal:  $B^{\text{new}} = (M^{\text{new}})^{-1}N^{\text{new}}$ , where

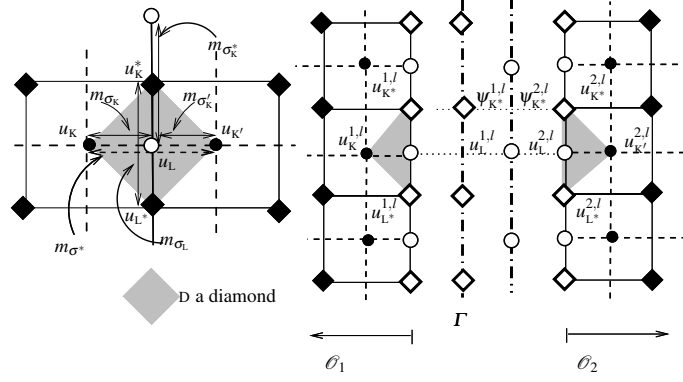


**Fig. 2** Notation around a diamond. The new unknowns needed to describe the DDFV scheme on  $\Omega$  as the limit of the Schwarz algorithm

$$M^{\text{new}} = \begin{pmatrix} \frac{1}{h}(1-\lambda) + \frac{p}{2}(1+\lambda) & 0 \\ 0 & \frac{1}{h}(1-\lambda) - \frac{\alpha_k}{2h} + p \end{pmatrix}$$

$$N^{\text{new}} = \begin{pmatrix} -\frac{1}{h}(1-\lambda) + \frac{p}{2}(1+\lambda) & 0 \\ 0 & -\frac{1}{h}(1-\lambda) + \frac{\alpha_k}{2h} + p \end{pmatrix},$$

and we obtain a much better convergence result.

**Proposition 2.** *The optimized parameter in the DDFV Schwarz algorithm ((3)-(8)) with modified traces (11) satisfies  $p_{\text{opt}} = \text{Argmin}_p \max_k (\rho(B^{\text{new}})) \sim \frac{2^{3/4} \sqrt{k_{\min}}}{\sqrt{h}}$ , and the associated optimized contraction factor is  $1 - 2^{1/4} \sqrt{k_{\min}} \sqrt{h} + O(h)$ .*

*Proof.* The proof of this result is based on equioscillation of the first eigenvalue of  $B^{\text{new}}$  at  $k = k_{\min}$  and the second eigenvalue of  $B^{\text{new}}$  at  $k = k_{\max} \approx \frac{\pi}{h}$ , using asymptotic analysis. The details are however too long for this short paper.

We now describe the DDFV Schwarz algorithm for general subdomains and decompositions using the notation from [3]. DDFV schemes can be described by two operators: a discrete gradient  $\nabla^{\mathcal{D}}$  and a discrete divergence  $(\text{div}_{\mathcal{K}}, \text{div}_{\mathcal{K}^*})$ , which are dual to each other, see [2] or [3]. We refer to the primal unknowns by  $u_{\mathcal{K}}^{j,l}$  or  $u_{\mathcal{L}}^{j,l}$ , to the dual unknowns by  $u_{\mathcal{K}^*}^{j,l}$  or  $u_{\mathcal{L}^*}^{j,l}$  and to the set of unknowns by  $u^{j,l}$ . The primal mesh on  $\Omega_j$  is called  $\mathfrak{M}_j$ , the dual mesh on  $\Omega_j$  is  $\mathfrak{M}_j^*$  for the interior cells,  $\partial\mathfrak{M}_{j,\Gamma}^*$  for the dual boundary cells related to  $\Gamma$  and the diamond mesh on  $\Omega_j$  is called  $\mathcal{D}_j$ . We further need additional unknowns  $u_{\mathcal{L}}^{j,l}$  on the edges of  $\Gamma$  denoted by  $\partial\mathfrak{M}_{j,\Gamma}$ , and additional fluxes  $\psi_{\mathcal{K}^*}^{j,l}$  for  $\mathcal{K}^* \in \partial\mathfrak{M}_{j,\Gamma}^*$  as shown in Figure (2). We denote by  $\mathcal{D}_{\mathcal{K}^*}$  the set of diamonds such that  $\mathcal{D} \cap \mathcal{K}^* \neq \emptyset$  for  $\mathcal{K}^* \in \partial\mathfrak{M}_{j,\Gamma}^*$ . The DDFV Schwarz algorithm then computes for  $l \in \mathbb{N}^*$ ,  $j = 1, 2$ ,  $i = 2, 1$

$$-\text{div}_{\mathcal{K}}(\nabla^{\mathcal{D}} u^{j,l}) = 0, \quad \forall \mathcal{K} \in \mathfrak{M}_j, \quad -\text{div}_{\mathcal{K}^*}(\nabla^{\mathcal{D}} u^{j,l}) = 0, \quad \forall \mathcal{K}^* \in \mathfrak{M}_j^*, \quad (12a)$$

$$- \sum_{D \in \mathfrak{D}_{K^*}} m_{\sigma^*} \left( \nabla^{\mathfrak{D}} u^{j,l}, \mathbf{n}_{\sigma_{K^*}} \right) - m_{\sigma_{K^*}} \psi_{K^*}^{j,l} = 0, \quad \forall K^* \in \partial \mathfrak{M}_{j,\Gamma}^*, \quad (12b)$$

$$\left( \nabla^{\mathfrak{D}} u^{j,l}, \mathbf{n}_{ji} \right) + p u_L^{j,l} = - \left( \nabla^{\mathfrak{D}} u^{i,l-1}, \mathbf{n}_{ij} \right) + p u_L^{i,l-1}, \quad \forall L \in \partial \mathfrak{M}_{j,\Gamma}, \quad (12c)$$

$$\psi_{K^*}^{j,l} + p u_{K^*}^{j,l} = - \psi_{K^*}^{i,l-1} + p u_{K^*}^{i,l-1}, \quad \forall K^* \in \partial \mathfrak{M}_{j,\Gamma}^*. \quad (12d)$$

Using the same discrete Fourier transform for (12) as in Section (2), we obtain  $B^{\text{new}}$ . Well-posedness of the algorithm can be proved using classical a priori estimates with the discrete duality property.

**Theorem 1 (Convergence of the new Schwarz algorithm).** *For all  $p > 0$ , the solution of the new Schwarz algorithm (12) converges as  $l$  tends to infinity to the solution of the classical DDFV scheme for the Laplace equation on  $\Omega$ .*

*Proof.* We first rewrite the classical DDFV scheme for the Laplace equation on  $\Omega$  as the limit of the Schwarz algorithm. To this end, we introduce new unknowns near the boundary  $\Gamma$ , see Figure (2):

- for all  $K \in \mathfrak{M}_j$ , we set  $u_K^{j,\infty} = u_K$  and for all  $K^* \in \mathfrak{M}_j^*$ , we set  $u_{K^*}^{j,\infty} = u_{K^*}$ ,
- for all  $L \in \partial \mathfrak{M}_{j,\Gamma}$  choose  $u_L^{j,\infty} = u_L^{i,\infty} = \frac{m_{\sigma_{K'} u_K + m_{\sigma_K} u_{K'}}}{m_{\sigma^*}}$ ,
- for all  $K^* \in \partial \mathfrak{M}_{j,\Gamma}^*$  choose  $u_{K^*}^{j,\infty} = u_{K^*}^{i,\infty} = u_{K^*}$  and

$$\psi_{K^*}^{j,\infty} = - \psi_{K^*}^{i,\infty} = - \frac{1}{m_{\sigma_{K^*}}} \sum_{D \in \mathfrak{D}_{K^*}} m_{\sigma^*} \left( \nabla^{\mathfrak{D}} u^{j,\infty}, \mathbf{n}_{\sigma_{K^*}} \right).$$

By linearity it suffices to prove the convergence of the new DDFV Schwarz algorithm (12) to zero. An a priori estimate using discrete duality leads to

$$2 \sum_{D \in \mathfrak{D}_j} m_D \|\nabla^{\mathfrak{D}} u^{j,l+1}\|^2 - \sum_{L \in \partial \mathfrak{M}_{j,\Gamma}} m_{\sigma_L} \left( \nabla^{\mathfrak{D}} u^{j,l+1}, \mathbf{n}_{\sigma_L} \right) u_L^{j,l+1} - \sum_{K^* \in \partial \mathfrak{M}_{j,\Gamma}^*} m_{\sigma_{K^*}} \psi_{K^*}^{j,l+1} u_{K^*}^{j,l+1} = 0.$$

We now rewrite the last two terms as

$$\begin{aligned} - \sum_{L \in \partial \mathfrak{M}_{j,\Gamma}} m_{\sigma_L} \left( \nabla^{\mathfrak{D}} u^{j,l+1}, \mathbf{n}_{\sigma_L} \right) u_L^{j,l+1} &= \frac{1}{4p} \sum_{L \in \partial \mathfrak{M}_{j,\Gamma}} m_{\sigma_L} \left( - \left( \nabla^{\mathfrak{D}} u^{j,l+1}, \mathbf{n}_{\sigma_L} \right) + p u_L^{j,l+1} \right)^2 \\ &\quad - \frac{1}{4p} \sum_{L \in \partial \mathfrak{M}_{i,\Gamma}} m_{\sigma_L} \left( - \left( \nabla^{\mathfrak{D}} u^{i,l}, \mathbf{n}_{\sigma_L} \right) + p u_L^{i,l} \right)^2, \end{aligned}$$

and using (12b)

$$\begin{aligned} &- \sum_{K^* \in \partial \mathfrak{M}_{j,\Gamma}^*} m_{\sigma_{K^*}} \psi_{K^*}^{j,l+1} u_{K^*}^{j,l+1} \\ &= \frac{1}{4p} \sum_{K^* \in \partial \mathfrak{M}_{j,\Gamma}^*} m_{\sigma_{K^*}} \left( p u_{K^*}^{j,l+1} - \psi_{K^*}^{j,l+1} \right)^2 - \frac{1}{4p} \sum_{K^* \in \partial \mathfrak{M}_{i,\Gamma}^*} m_{\sigma_{K^*}} \left( p u_{K^*}^{i,l} - \psi_{K^*}^{i,l} \right)^2. \end{aligned}$$

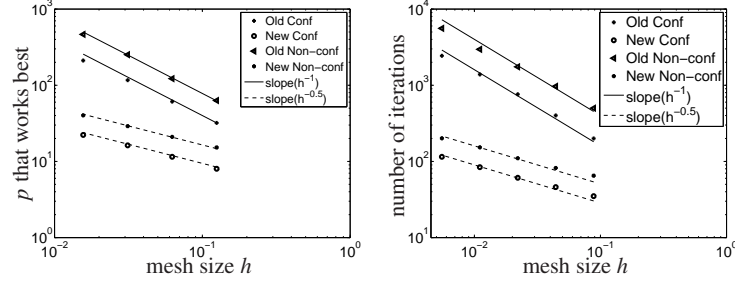


**Fig. 3** Asymptotic behavior of the numerically optimized parameter  $p$  on the left, and number of iterations to reduce the error by a factor of  $10^{-10}$  on the right

Summing over  $l = 0, \dots, l_{max} - 1$  and  $j = 1, 2$ , we get

$$\begin{aligned}
& 2 \sum_{l=0}^{l_{max}-1} \sum_{j=1,2} \sum_{D \in \mathcal{D}_j} m_D \|\nabla^{\mathcal{D}} u^{j,l+1}\|^2 + \frac{1}{4p} \sum_{j=1,2} \sum_{L \in \partial \mathcal{M}_{j,\Gamma}} m_{\sigma_L} \left( p u_L^{j,l_{max}} - (\nabla^{\mathcal{D}} u^{j,l_{max}}, \mathbf{n}_{\sigma_L}) \right)^2 \\
& + \frac{1}{4p} \sum_{j=1,2} \sum_{K^* \in \partial \mathcal{M}_{j,\Gamma}^*} m_{\sigma_{K^*}} \left( -\psi_{K^*}^{j,l_{max}} + p u_{K^*}^{j,l_{max}} \right)^2 \\
& = \sum_{j=1,2} \frac{1}{4p} \left( \sum_{L \in \partial \mathcal{M}_{j,\Gamma}} m_{\sigma_L} \left( -(\nabla^{\mathcal{D}} u^{j,0}, \mathbf{n}_{\sigma_L}) + p u_L^{j,0} \right)^2 + \sum_{K^* \in \partial \mathcal{M}_{j,\Gamma}^*} m_{\sigma_{K^*}} \left( -\psi_{K^*}^{j,0} + p u_{K^*}^{j,0} \right)^2 \right).
\end{aligned}$$

This shows that the total energy stays bounded as the iteration  $l$  goes to infinity, and hence the algorithm converges.

## 4 Numerical experiments

We show results for Laplace's equation on  $\Omega = (-1, 1)^2$  with two subdomains  $x > 0$  and  $x < 0$ . We first simulate in Figure (3) the error equations, i.e. using homogeneous data, and starting with a random initial guess. On the left, we show the  $p$  that worked best as  $h$  is refined, both for a conforming square mesh ( $2^i \times 2^i$  squares on  $\Omega_j$ ,  $j = 1, 2$ ), and for a non-conforming square mesh ( $2^i \times 2^i$  squares on  $\Omega_1$  and  $3^i \times 3^i$  squares on  $\Omega_2$ ). On the right, we show the number of iterations needed to get an error reduction of  $10^{-10}$ . These experiments illustrate well our theoretical results.

We next show a case with exact solution  $u(x, y) = \cos(2.5\pi x) \cos(2.5\pi y)$ . Starting with a random initial guess, Figure (4) shows the convergence history of the algorithms for various parameters  $p$  on the left, and snapshots of the error at iteration 10 on the right. We clearly see that for  $p$  too small, high frequencies dominate the error, and for  $p$  large low frequencies. In the old algorithm, the theoretically optimized choice  $p = 90.5$ , and in the new algorithm the theoretically optimized choice  $p = 14.18$  will work best in the long run. Finally, a priori knowledge of the

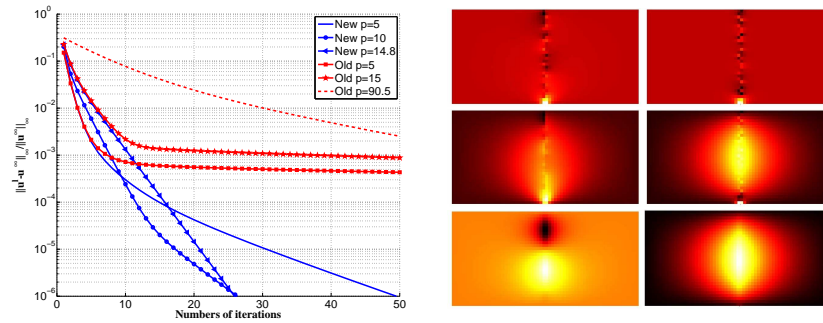


**Fig. 4** Left: convergence history on a conforming  $32 \times 32$  square mesh. Right: snapshots of the error at iteration 10, left column for the old version and  $p = 5, 15, 90.5$ , right column for the new version and  $p = 5, 10, 14.18$

frequency content of the solution can be used to choose a  $p$  that gives very rapid convergence early on in the iteration (here  $p = 5$ , good for low frequencies). This choice becomes however very bad in the long run, once other error frequencies become important.

## References

1. Achdou, Y., Japhet, C., Nataf, F., Maday, Y.: A new cement to glue non-conforming grids with Robin interface conditions: The finite volume case. *Numer. Math.* **92**(4), 593–620 (2002)
2. Andreianov, B., Boyer, F., Hubert, F.: Discrete duality finite volume schemes for Leray-Lions type elliptic problems on general 2D-meshes. *Num. Meth. for PDEs* **23**(1), 145–195 (2007)
3. Boyer, F., Hubert, F., Krell, S.: Non-overlapping Schwarz algorithm for solving 2d m-DDFV schemes. *IMA Jour. Num. Anal.* **30** (2009)
4. Cautrès, R., Herbin, R., Hubert, F.: The Lions domain decomposition algorithm on non-matching cell-centred finite volume meshes. *IMA J. Numer. Anal.* **24**(3), 465–490 (2004)
5. Coudière, Y., Pierre, C.: Stability and convergence of a finite volume method for two systems of reaction-diffusion equations in electro-cardiology. *Nonlinear Anal. R. World Appl.* **7**(4), 916–935 (2006)
6. Domelevo, K., Omnes, P.: A finite volume method for the Laplace equation on almost arbitrary two-dimensional grids. *M2AN Math. Model. Numer. Anal.* **39**(6), 1203–1249 (2005)
7. Dubois, O.: Optimized Schwarz methods for the advection-diffusion equation and for problems with discontinuous coefficients. Ph.D. thesis, McGill University, Canada (June 2007)
8. Gander, M.J.: Optimized Schwarz method. *SIAM J. on Numer. Anal.* **44**(2), 699–731 (2006)
9. Gander, M.J., Japhet, C., Maday, Y., Nataf, F.: A new cement to glue nonconforming grids with Robin interface conditions: the finite element case. *Lect. Notes Comput. Sci. Eng.* **40**, 259–266 (2005)
10. Gerardo-Giorda, L., Nataf, F.: Optimized schwarz methods for unsymmetric layered problems with strongly discontinuous and anisotropic coefficients. *J. Numer. Math.* **13**, 265–294 (2005)
11. Herbin, R., Hubert, F.: Benchmark on discretization schemes for anisotropic diffusion problems on general grids. In: R. Eymard, J.M. Hérard (eds.) *Proceedings of FVCA V*. Hermès (2008)
12. Lions, P.L.: On the Schwarz alternating method. III. A variant for nonoverlapping subdomains. In: *Third International Symposium on DDM* (Houston, 1989), pp. 202–223. SIAM (1990)